IN-20
79976

NASA Technical Memorandum 105578

P.20

Neutralizer Optimization

Michael J. Patterson
Lewis Research Center
Cleveland, Ohio

and

Kayhan Mohajeri
Purdue University
West Lafayette, Indiana

Prepared for the
22nd International Electric Propulsion Conference
cosponsored by the AIDAA, AIAA, DGLR, and JSASS
Viareggio, Italy, October 14–17, 1991

NASA

(NASA-TM-105578) NEUTRALIZER OPTIMIZATION (NASA) 20 p CSCL 21H

N92-21976

Unclas

G3/20 0079976

NEUTRALIZER OPTIMIZATION

Michael J. Patterson*
National Aeronautics and Space Administration
Lewis Research Center

Kayhan Mohajeri†
Department of Physics
Purdue University

This paper discusses the preliminary results of a test program to optimize a neutralizer design for 30 cm xenon ion thrusters. The impact of neutralizer geometry, neutralizer axial location, and local magnetic fields on neutralizer performance is discussed. The effect of neutralizer performance on overall thruster performance is quantified, for thruster operation in the 0.5-3.2 kW power range. Additionally, these data are compared to data published for other NSSK and primary propulsion xenon ion thruster neutralizers.

Introduction

The neutralizer is a key element in the functional operation of an ion engine, and it's efficient operation is important to a host of thruster issues including performance (efficiency, specific impulse, stability, reliability, etc.) and lifetime. Ion thruster neutralizer technology has evolved to the development of the hollow cathode plasma bridge device as the optimal approach to thruster beam neutralization. Plasma bridge neutralizer technology for mercury ion thrusters was developed to a high state of maturity[1-3], and included a successful flight experiment which demonstrated it's operation both as an effective means of beam neutralization and spacecraft potential control.[4-6]

For nearly a decade, the emphasis both in the United States and elsewhere has been toward the development of xenon ion thrusters, for both auxiliary and primary propulsion. This activity has included, in the U.S., the development of an advanced engineering model 25 cm ion thruster.[7] This thruster, and associated plasma bridge neutralizer, successfully completed a 4350-hour cyclic lifetest in 1987, at a design input power level of 1.3 kW.[8] The development activity associated with the plasma bridge neutralizer for this thruster represents the only large body of work conducted on xenon neutralizers in the U.S. to date. Other data for xenon, and other inert gas, neutralizers are limited and do not reflect optimization efforts. These data include mechanical or feed system induced failures of neutralizer assemblies during the only two high power xenon ion thruster weartests conducted to date.[9,10] In addition, for at least one of these tests, a high erosion rate of the neutralizer assembly was experienced due to direct beam interception.[10] For these reasons a neutralizer optimization activity for high power xenon ion thrusters would appear warranted.

Recently, a program was initiated at NASA-Lewis Research Center (LeRC) to develop a "derated" ion engine which is a light-weight (~7 kg) engineering model 30 cm xenon ion thruster designed to operate over a broad range of input power levels (~0.5-5.0 kW) and beam currents appropriate to both auxiliary and primary propulsion functions. Test data and analyses indicate that this type of approach may provide significant operations and reliability

*Aerospace Engineer, member AIAA.
†Undergraduate student.

advantages over that of the conventional small thruster approach to auxiliary propulsion.[11,12] Because the performance advantage of the derated ion concept relies on operation at a higher beam current than that of the smaller thrusters for a fixed input power, this may incur higher penalties in terms of neutralizer propellant and power expenditures. Consequently, it is appropriate to optimize neutralizer performance, and address issues associated with throttling and scalability of this component on the derated thruster.

To this end, an activity to develop xenon plasma bridge neutralizer technology has been initiated, preliminary results of which are presented here. Additionally, these results are compared to the state-of-the-art of xenon neutralizer development elsewhere.

Apparatus and Procedure

For this investigation, several laboratory-version neutralizer assemblies were fabricated. The initial mechanical design for the neutralizer experiments (shown in Fig. 1a) was similar to the high performance design developed at Hughes Research Laboratories for the 25 cm Xenon Ion Propulsion System (XIPS) thruster.[7,8,13] The only substantiative modification made to the initial geometry reported here, from that of the XIPS design, was the elimination of the permanent magnets. This was done because it was identified that the magnetic augmentation did not appreciably improve the neutralizer performance.[14] Additional modifications, which were not believed to impact neutralizer performance, were made from that of the XIPS design to ease fabrication, assembly, and disassembly. Subsequent modifications from the baseline neutralizer design, shown in Figs. 1b-c and listed in Table I, were made to improve performance and are discussed in the Results and Discussion section.

The neutralizer design depicted in Fig. 1a consists of a hollow cathode assembly, keeper electrode, insulators and clamping fixture, and an external housing. The hollow cathode assembly consists of a molybdenum-rhenium alloy tube of 0.64 cm external diameter, with a 2-percent thoriated tungsten orifice plate electron-beam welded to one end. The orifice plate has a centered 0.51 mm hole discharge machined through the thickness dimension, with a 45-degree half angle chamfer on the downstream surface of the orifice wall. The thickness of the orifice plate is approximately 0.13 cm, with the chamfer pentrating to a depth of approximately 0.51 mm. Internal to the hollow cathode tube is a porous tungsten insert impregnated with a low-work function compound to serve as the source of electrons. The insert is butted against the rear of the orifice plate, and secured by mechanical attachment of the insert electrical leads to the upstream end of the tube. External to the downstream end of the cathode is a swaged heater friction-fitted to the tube body, used for insert activation and cathode starting. This hollow cathode assembly geometry was used for all the testing conducted in this investigation.

The neutralizer keeper electrode consists of a molybdenum tube of approximately 1.7 cm internal diameter, positioned concentric with the hollow cathode tube. The end of the keeper electrode is approximately 1.9 cm downstream of the hollow cathode tube. External to the cathode and keeper electrodes is the assembly housing, which consists of a stainless steel cylindrical tube of nominal 3.8 outside diameter, with a molybdenum orifice plate secured to the downstream end of the tube. The molybdenum orifice plate has a thickness of approximately 0.14 cm, with a centered aperture of 0.64 cm diameter. The external housing acts as a pressure vessel to reduce the neutral loss rate, and provides for a mechanical attachment of the neutralizer cathode assembly to the thruster. For all tests, the neutralizer assembly centerline was located 8.9 cm radially outward from the outermost apertures of the accelerator grid; a location relative to the ion beam identified as optimal during the mercury ion thruster development program.[3] The exterior housing of the neutralizer assembly was mechanically and electrically tied to the exterior plasma screen of the ion thruster.

Experiments to characterize the operation and performance of various neutralizer geometries were conducted in conjunction with the operation of a 30 cm diameter laboratory model ion thruster. The thruster, described in reference 11, incorporates a ring-cusp discharge chamber, and conventional two-grid ion optics. All neutralizer experiments except for those involving axial translation of neutralizer assembly, utilized this thruster. The translation experiments used a similar design thruster (described in ref. 10), which more readily permitted mechanical modification to the neutralizer-thruster housing interface.

The thruster was operated with standard laboratory power supplies (described in ref. 10), requiring four for steady-state operation, including one for the neutralizer keeper operation. Additional heater power supplies for the discharge and neutralizer cathodes, were used for starting only. All power supplies were electrically isolated from facility ground to insure correct neutralization of the ion beam. Neutralizer coupling voltage was measured, and is defined here as the potential difference between neutralizer-common and facility ground. Fogure 2 shows an electrical schematic of the experiment. A zener diode was used to limit the maximum floating potential of neutralizer common to approximately -70 volts. Provision was made for floating or grounding the engine plasma screen and neutralizer exterior housing via external switch.

All propellant lines including that for the neutralizer, incorporated individual mass flow transducers to measure the propellant flow rate to the thruster. Prior to testing the transducers were calibrated on xenon using a primary standard.

Nominal ion thruster operating conditions, chosen for neutralizer optimization experiments, are identified in Table II. These conditions ranged from 0.8 A to 1.45 A beam current - corresponding to thruster input power levels of from approximately 670 W to 1620 W.

All testing was conducted at the NASA-LeRC tank 5 vacuum chamber. The facility, approximately 4.6 m in diameter and 19.2 m long, utilizes oil diffusion pumps to operate at a nominal pumping speed of approximately 90,000 ℓ/s xenon.

Results and Discussion

This section presents results obtained from neutralizer optimization activities, a discussion of the impact of neutralizer performance on overall thruster performance, and a comparative assessment of the neutralizer results obtained in this investigation with those published elsewhere.

Neutralizer Optimization

Experiments to optimize neutralizer performance included assessing the impact of mechanical and electrical design modifications to the baseline geometry (identified in Fig. 1a), axial position of the neutralizer with respect to the thruster ion beam, and stray magnetic fields in the region of the neutralizer assembly.

Geometry - In these experiments, the position of the neutralizer hollow cathode orifice plate remained fixed with respect to the ion thruster at a location approximately 0.8 cm downstream of the axial location of the outermost accelerator grid apertures; a position referred henceforth as the standard location. For the initial geometry tested (Fig. 1a), this meant that the neutralizer assembly housing was located approximately 3.2 cm downstream of the axial location of the outermost holes of the accelerator grid electrode. The radial location of the assembly centerline was 8.9 cm from the outermost apertures in the accelerator grid electrode. A total of four neutralizer geometries were characterized, as indicated in Table I.

Initial testing of the neutralizer geometry shown in Fig. 1a (henceforth referred to as geometry #1) was conducted with the assembly housing and thruster plasma screen electrically tied to facility ground. During these experiments the coupling voltage was found to be insensitive to neutralizer propellant flow, and it was speculated that neutralizer emission was to the grounded exterior housing, and the thruster ion beam was current neutralized via ground return circuit and charge neutralized via secondary electron emission from the beam target. Consequently, the thruster was modified to allow the neutralizer exterior housing and plasma screen to be electrically isolated from facility ground.

Figure 3 shows coupling voltage versus flow rate data obtained with neutralizer geometry #1, at a xenon ion beam current of 1.45 A, and a fixed neutralizer keeper current of 2.0 A. Data with the assembly housing and plasma screen grounded and floating are shown. As indicated, a considerable difference in coupling voltage is observed under these two conditions. A calibrated current probe was used to measure the electron current to the grounded neutralizer exterior housing and plasma screen, and a value equal to that of the beam current was observed. These two conditions are shown schematically in Figs. 2 and 4. Under the grounded condition the neutralizer emission coupled directly to the exterior housing orifice plate, while under the floating condition the neutralizer emission coupled to the ion beam.

As indicated in Fig. 3, the coupling voltage for this neutralizer geometry asymptotically approaches -20 volts, at a xenon flow rate of 400 mA; a flow rate nearly equal to 30 percent of that of the beam. Additional data for geometry #1 are shown in Fig. 5. Figure 5 indicates that for a fixed flow rate, the coupling voltage is insensitive to beam current in the 0.8 to 1.45 A range. To obtain a coupling voltage $<$ 25 volts at 0.80 A beam current, nearly one-third of the propellant flow rate into the thruster would have to be diverted to the neutralizer. An additional datum point reported for the Hughes neutralizer is plotted on Fig. 4, obtained at a beam current of 1.45 A.[8] The near order-of-magnitude difference in neutralizer flow rate between that of geometry #1 and that reported for the XIPS thruster remains unresolved. The neutralizer keeper voltages for both geometry #1 and the XIPS assembly are shown in Fig. 6 for the indicated beam currents.

The performance of neutralizer geometry #1 (under the condition of a floating housing) was considered unacceptable from both a standpoint of coupling voltage and propellant flow rate; consequently an activity was initiated to improve its performance. The first modification made to the baseline geometry, referred to here as geometry #2, was to simply remove the molybdenum orifice plate from the external housing as shown in Fig. 1b. Data for this geometry are shown in Figs. 7 and 8, plots of both coupling and keeper voltage as functions of neutralizer flow rate. Typical coupling and keeper voltages were -32 V and 15 V, respectively, at 400 mA xenon flow rate. These data indicate a degradation in performance from that obtained with geometry #1. This may have been anticipated, as removal of the orifice plate reduced the internal pressure and increased the neutral loss rate. Operating this geometry with the external housing and plasma screen grounded, a current equal to 34 percent of the beam current was measured to ground, with the remainder coupling into the ion beam.

At this juncture it was felt appropriate to make a radical departure in mechanical design from that of geometry #1. The baseline geometry was modified by removing the molybdenum orifice plate and machining back the external housing behind the keeper tube, so that the housing served only as a point of mechanical attachment to the thruster. Additionally the keeper tube length was shortened, and a molybdenum keeper cap was machined and installed on the tube to form an "enclosed-keeper" geometry. The keeper-to-neutralizer orifice plate gap, and the keeper orifice diameter were set at 0.13 cm and 0.47 cm, respectively, comparable to that used in the J-series mercury ion thruster neutralizer assembly.[15] This assembly, designated as geometry #3, is shown in Fig. 1c.

Data from this geometry are presented in Figs. 9 and 10, plots of coupling and keeper voltages versus flow rate. As indicated, the magnitude of the coupling voltage can be reduced to less than 20 V are obtainable at xenon flow rates $>$ 200 mA. Coupling voltages in the range of -20 to -25 V are observed for flow rates in the range of 150-200 mA at the indicated beam currents. The performance for this geometry represents a significant (~2.0-2.7x) reduction in flow rate from that required for geometries #1 and #2. The flow rates, corresponding to the knee of the coupling voltage-flow rate curves, are however fairly insensitive to beam current. Consequently the required neutralizer flow rate represents a larger fraction of the total propellant flow rate to the thruster at lower power levels. Measured as a ratio of beam current to neutralizer flow rate in equivalent amperes, geometry #3 operates at a ratio of ~6.4 and ~9.7 at beam currents of 0.8 A and 1.45 A, respectively. Under the condition of a grounded plasma screen, a current equal to ~10 percent of the beam current was measured to ground through the plasma screen, concurrent with a reduction in the magnitude of the coupling voltage of approximately 5 volts.

In an attempt to further reduce the neutralizer flow rate requirement, the keeper orifice was reduced from 0.47 cm to 0.33 cm diameter. Data for this geometry, designated geometry #4, are shown in Figs. 11 and 12. Although this design resulted in lower keeper voltages than observed with geometry #3, an increase in minimum coupling voltage was suffered for the same beam current. It is hypothesized that the reduction in keeper voltage is associated with the higher neutral density (lower neutral loss rate, and higher ionization rate with the smaller orifice), while the increase in coupling voltage is due to the increased keeper surface area which increased the ion loss area for recombination (hence, a lower density cold ion population emitted by the neutralizer).

To summarize the neutralizer performance results, the coupling and keeper voltages for all four geometries are presented in Figs. 13 and 14 at 1.45 A beam current. As indicated, the lowest coupling voltages were experienced with geometry #3. Typical performance for this geometry was -25 V coupling voltage, at 200 mA xenon flow rate, at a keeper voltage and current of 14 volts and 2.0 amperes, respectively.

Axial Location - To assess the impact of axial position on neutralizer coupling voltage, a mechanical assembly was attached to the upstream end of neutralizer geometry #1 to permit in-situ translation of the neutralizer with respect to the thruster and ion beam. For these tests the centerline of the neutralizer assembly was again at a radial location of 8.9 cm with respect to the accelerator grid electrode. The range of motion for the neutralizer assembly (as measured at the assembly housing orifice plate) was from 1.9 cm to 9.6 cm downstream of the axial location of the outermost accelerator grid apertures. These axial locations correspond to angles of 78 and 43 degrees made between the beam axis normal to the grid plane, and the front tip of the neutralizer exterior housing.

The coupling voltage-flow rate characteristics obtained for this configuration are shown in Fig. 15. There was no discernable impact of axial location on the coupling voltage, going from the fully-retracted position of 1.9 cm to the fully-extended position of 9.6 cm. This performance insensitivity to axial position is of benefit in terms of flexibility in thruster mechanical design, permitting the neutralizer assembly to be outside an envelope for direct ion beam interception and erosion by high-angle ions. These data are consistent with that reported elsewhere for a 30 cm mercury thruster which showed little variation of coupling voltage with axial position.[16]

Stray Magnetic Fields - An experiment was conducted to assess the impact of stray magnetic fields on neutralizer coupling. This experiment was motivated by the following considerations: (1) a previous investigation had concluded that magnetic fields in the region of the neutralizer cathode orifice as low as a 0.1 mT can adversely effect the neutralizer coupling process[17]; (2) flux density measurements made exterior to surfaces of several laboratory model ring-cusp ion thrusters identified volume fields as high as 2.5 mT[18], which are comparable to the flux densities observed in the discharge chamber of the J-series ion thruster; and (3) recent experiments with ring-cusp ion thrusters indicate that use of a steel chamber to carry the return flux is not essential in obtaining high discharge performance[18], however the exclusive use of non-magnetic chamber materials without shielding will increase the exterior fringe fields.

Measurements of the axial component of the magnetic flux density in the region of the neutralizer cathode assembly were made with geometry #2 and are shown in Fig. 16. These data were obtained along the neutralizer assembly centerline from the plane of the hollow cathode orifice to a position approximately 12 cm downstream, at the standard position previously identified. As indicated, the axial field component at the hollow cathode orifice plate was ~1.1 mT. Adding two permanent magnets on the surface of the plasma screen between the thruster and the neutralizer assembly housing, a reduction in the axial field component could be effected, as indicated in Fig. 16. The impact of reducing the axial magnetic flux density at the cathode orifice from ~1.1 mT to ~0 mT on neutralizer coupling voltage is shown in Fig. 17. A reduction in coupling voltage of approximately 15 volts or more was effected for a given low flow rate.

Based on this experience, an electromagnet assembly was fabricated to permit in-situ variation of the axial flux density along the axis of the neutralizer assembly. An electromagnet consisting of 36 turns of 16 gauge wire wound around a 3.8 cm diameter stainless steel cylindrical tube was constructed and installed on the downstream end of neutralizer geometry #3. The electromagnet, friction-fitted to the neutralizer assembly tube, was machined to be concentric to the hollow cathode body tube. Additionally, the orifice plate of the hollow cathode was located axially at the geometric center of 7.6 cm long electromagnet.

The variations in axial magnetic flux density as a function of applied eletromagnet current, at the plane of the neutralizer keeper and electromagnet exit plane, are shown in Fig. 18. As indicated, maximum axial fields of ~3.5 mT and ~ 0.4 mT were obtained at the keeper and exit plane, respectively, for a 4 A applied current.

Figure 19 shows the variation in coupling and keeper voltages with eletromagnet current for a thruster beam current of 1.45 A, and a neutralizer flow rate of approximately 220 mA. The coupling voltage varied from approximately -28 V at 0.25 A electromagnet current, to -13 V for electromagnet currents from 2 to 8 amperes. This transition corresponds to a near-doubling of the axial flux density from approximately 1 to 2 mT at the plane of the neutralizer keeper. Although the mechanism for the reduction in coupling voltage is not presently understood, it is of interest to note that the gyroradius for 20 eV electrons at 1 mT, 1.5 cm, is approximately equal to the radius of the electromagnet tube, and drops to less than half this value for applied currents greater than 2 amperes. An increase in keeper voltage was experienced with increasing electromagnet current; this trend continued upwards to 20 volts at a peak applied current of 8 amperes.

These results indicate that magnetic fields in the region of the neutralizer assembly can impact the neutralizer coupling voltage. While the data obtained with the permanent magnets and the electromagnet assembly appear somewhat disparate, a direct comparison may not be feasible. As for example, the physical presence of the electromagnet assembly alone, without an applied current, resulted in an increase in coupling voltage of approximately 7 volts, from that obtained without the assembly. Further investigation is warranted.

Impact on Thruster Performance

The performance of the plasma bridge neutralizer can impact the overall steady-state thruster performance in several ways: (1) the power consumed by the neutralizer keeper {and heater, if not self-heating} represents a power loss which reduces the electrical efficiency and hence overall thruster efficiency; (2) the coupling power (the product of the coupling voltage and beam current) reduces the electrical efficiency, hence overall thruster efficiency for a fixed beam voltage; and (3) the propellant flow rate required of the neutralizer cathode reduces the propellant utilization efficiency, hence thruster specific impulse and efficiency.

The total power requirement of the neutralizer can be expressed as:

$$P_{neut} = J_{nk} \cdot V_{nk} + J_{nh} \cdot V_{nh} + |V_g| \cdot J_b$$

where J_{nk} and V_{nk} are the keeper current and voltage, J_{nh} and V_{nh} are the heater current and voltage, V_g is the coupling voltage, and J_b is the beam current. For a proper thermal design neutralizer cathode, the heater term will be zero for steady-state operation.

From a thruster performance consideration, the optimal neutralizer operating point is that which maximizes both the neutralizer power and propellant efficiency. However, as is the case for thruster discharge chamber performance, these conditions cannot be simultaneously satisfied. Consequently, a compromise in power and propellant efficiencies is necessary. An optimal neutralizer operating condition can be identified from the 'knee' of the plot of the neutralizer power required per beam electron current versus the ratio of neutralizer beam electron current to neutral flow rate (neutral flow rate in equivalent amperes). These characteristics, for geometry #3 neutralizer, are shown in Fig. 20, for beam currents of 1.20 and 1.45 amperes. As indicated, a nominal performance of ~50 watts per beam electron ampere at a ratio of ~9 beam electrons per neutral gas atom was obtained. Projected performance for a reduced-size cathode orifice (permitting a reduction in keeper current to 1.0 A) is also shown. Lifetime constraints will also need to be imposed on the neutralizer operating condition by identifying maximum acceptable levels of emission current, and keeper and coupling voltages to fully characterize and select the desired operating condition.

The magnitude of the impact of neutralizer performance on the overall performance of the derated ion thruster can be readily quantified. The power and mass flow rate requirements of the neutralizer are proportional to the total electron emission current requirement. The electron emission requirement is in turn directly proportional to the thruster beam ion current. Consequently the greatest sensitivity of thruster performance to neutralizer performance occurs when the thruster is operated at the maximum ratio of beam current-to-input power, or equivalently, the maximum ratio of thrust-to-power.

Figure 21 plots the percent reduction in thruster specific impulse and efficiency, due to neutralizer performance over a thruster input power range of approximately 550-to-3200 W. The nominal performance parameters of Fig. 20 for neutralizer geometry #3 were assumed. As indicated, the neutralizer degrades the specific impulse by approximately 9 percent over the total input power envelope because of its mass flow rate requirement, and thereby reduces the overall thruster efficiency by the same magnitude. The neutralizer power requirement also reduces the overall thruster efficiency. The combined efficiency reduction due to the required power and propellant expenditures for the neutralizer is shown in Fig. 21. As indicated, the efficiency reduction increases with decreasing thruster input power, going from approximately 14 percent at 3200 W, to 17 percent at 550 W. This is because the fraction of total thruster input power going into the neutralizer increases from approximately 5 to 10 percent as the thruster is throttled down to 550 W.

The neutralizer performance impact indicated in Fig. 21 represents a worst-case scenario because the thruster was operated at a condition requiring the maximum neutralizer emission current. Assuming a fixed keeper current of only 1 A, the broadest possible range in required total neutralizer electron emission current in the power envelope of 550 W to 3200 W will be 1.8-to-4.4 A. This range in current requirement can be adequately satisfied by a single neutralizer geometry.

Comparative Assessment

It is of interest to compare the performance of neutralizer geometry #3 to that of state-of-the-art xenon neutralizers developed elsewhere. Since each neutralizer assembly was optimized for a specific thruster and hence level of beam current, it is value to compare performance at the same total electron emission current (sum of beam electron and keeper currents). Figures 22 and 23 show the neutralizer mass flow rate requirement and input power requirement as functions of total neutralizer electron emission current, respectively, for several xenon neutralizers. Xenon neutralizer data from the MELCO[19], NAL[20], UK10[21], and RIT10[22,23] thrusters are presented, as well as data for the XIPS 25 cm[8], the J-series[24], and 5 kW and 10 kW weartest laboratory model thrusters.[9,10] A linear correlation exists between flow rate and total emission current. Most of the neutralizer geometries plotted in Fig. 22 operate at ratios of electron-to-neutral atom emission in the range of 15-to-35, with the notable exception of the XIPS neutralizer at ~53. A linear correlation exists as well for neutralizer power vs. emission current, as indicated in Fig. 23. All xenon neutralizer geometries plotted operate within a range of 15-to-20 watts input power per ampere of electron emission current. As indicated in both plots, neutralizer geometry #3 performance correlates with other devices. The data of Figs. 22 and 23 would suggest that significant improvements in xenon neutralizer performance may not be obtainable, as most geometries have undergone a high degree of optimization at their respective design operating points.

Recommendations

Recommended areas for additional neutralizer work include:

- a more quantitative assessment of the impact of stray magnetic fields and neutralizer location on neutralizer beam coupling, replete with beam and plasma diagnostics
- an assessment of the impact of neutralizer operation and location on charge-exchange ion production, and accelerator grid drain current and wear
- an assessment of the impact of background pressure on beam potential and neutralizer coupling voltage
- a correlation of neutralizer critical component erosion with neutralizer operating parameters
- demonstration of simple approaches to neutralizer voltage and flow control

Conclusions

Preliminary experimental results to optimize a xenon neutralizer design for 30 cm ion thrusters were presented.

The following conclusions are drawn from this activity:

- Isolating the ion thruster plasma screen from facility ground appears critical in effecting proper beam neutralization.

- Stray magnetic fields in the region of the neutralizer assembly appear to influence the ability of the neutralizer to couple into the ion beam efficiently.

- The performance of a baseline neutralizer geometry was insensitive to large variations in axial location with respect to the ion beam. This may permit a thruster design flexibility.

- A power expenditure of approximately 50 W per beam electron ampere, and an emission capability of aprroximately 9 beam electrons per neutral gas atom were demonstrated for an optimized neutralizer geometry. An additional improvement in performance is anticipated via reduction in cathode orifice diameter.

- The impact of the optimized neutralizer performance on overall thruster performance includes a ~9 percent reduction in specific impulse and a ~14-17 percent reduction in efficiency, over the input power range of 550-to-3200 W. The maximum variation in total neutralizer electron emission requirement of 1.8-to-4.4 A anticipated over this input power range may be achieved by a single neutralizer geometry.

- In general, state-of-the-art xenon neutralizers demonstrated here and elsewhere operate at comparable performance levels; 15-to-20 watts input power per total electron emission ampere, at ratios ranging from 15-to-35 in total electron-to-neutral current.

References

[1]Rawlin, V.K. and Pawlik, E.V., "A Mercury Plasma-Bridge Neutralizer," *J. Spacecraft and Rockets,* Vol. 5, No. 7, July 1968, pp. 814-820.

[2]Ward, J.W. and King, H.J., "Mercury Hollow Cathode Plasma Bridge Neutralizers," *J. Spacecraft and Rockets,* Vo. 5, No. 10, October 1968, pp. 1161-1164.

[3]Bechtel, R.T., "A Hollow Cathode Neutralizer for a 30-CM Diameter Bombardment Thruster," AIAA Paper No. 73-1052, October 1973.

[4]Jones, S.G., Staskus, J.V., and Byers, D.C., "Preliminary Results of SERT II Spacecraft Potential Measurements Using Hot Wire Emissive Probes," NASA TM X-2083, November 1970.

[5]Kerslake, W.R. and Domitz, S., "Neutralization Tests on the SERT II Spacecraft," AIAA Paper No. 79-2064, October 1979.

[6]Kerslake, W.R. and Ignaczak, L.R., "SERT II 1979-1981 Tests: Plasma Thrust and Neutralizer Measurements," *J. Spacecraft and Rockets,* Vol. 19, No. 3, May 1982, pp. 236-240.

[7]Beattie, J.R., et. al., "Xenon Ion Propulsion System," AIAA Paper No. 85-2012, September 1985.

[8]Beattie, J.R., Matossian, J.N., and Robson, R.R., "Status of Xenon Ion Propulsion Technology," AIAA Paper No. 87-1003, May 1987.

[9]Rawlin, V.K., "Internal Erosion Rates of a 10-kW Xenon Ion Thruster," AIAA Paper No. 88-2192, July 1988.

[10]Patterson, M.J. and Verhey, T.R., "5kW Xenon Ion Thruster Lifetest," AIAA Paper No. 90-2543, July 1990.

[11]Patterson, M.J. and Foster, J.E., "Performance and Optimization of a 'Derated' Ion Thruster for Auxiliary Propulsion," AIAA Paper No. 91-2350, June 1991.

[12]Rawlin, V.K. and Majcher, G., "Mass Comparison of Electric Propulsion Systems for NSSK of Geosynchronous Spacecraft," AIAA Paper No. 91-2347, June 1991.

[13]Beattie, J.R. and Matossian, J.N., "High-Power Xenon Ion Thrusters," AIAA Paper No. 90-2540, July 1990.

[14]Personal communication, Beattie, J.R., Hughes Research Laboratories, Malibu, CA, August 1990.

[15]Schnelker, D.E., et. al., "Characteristics of the NASA/Hughes J-Series 30-cm Engineering Model Thruster," AIAA Paper No. 79-2077, October 1979.

[16]Bechtel, R.T., "A Hollow Cathode Neutralizer for a 30-cm Diameter Bombardment Thruster," AIAA Paper No. 73-1052, October 1973.

[17]Feng, Yu-Cai and Wilbur, P.J., "The Influence of Strong Magnetic Fields on Ion Beam Neutralization," AIAA Paper No. 82-1945, November 1982.

[18]Patterson, M.J. and Rawlin, V.K., "Derated Ion Thruster Design Issues," IEPC 91-150, October 1991.

[19]Shimada, S., et. al., "Ion Engine System Development of ETS-VI," AIAA Paper No. 89-2267, July 1989.

[20]Kitamura, S., Miyazaki, K., and Hayakawa, Y., "1000 Hour Test of 14 cm Diameter Ring-Cusp Xenon Ion Thruster," AIAA Paper No. 90-2542, July 1990.

[21]Martin, A.R., Harvey, M.S., and Latham, P.M., "Performance Assessment of a UK Rare Gas Ion Thruster," *J. British Interplanetary Society,* Vol. 41, 1988, pp. 183-192.

[22]Bakker, K., Petagna, C., and Rohden, H.V., "Endurance Test of the RIT 10 Neutralizers," AIAA Paper No. 90-2545, July 1990.

[23]Bianconi, M., et. al., "A Review of the Manufacturing and Characterization Activities at PROEL of a Plasma Bridge Neutralizer for the RIT 10 Ion Thruster," AIAA Paper No. 90-25881, July 1990.

[24]Rawlin, V.K., "Operation of the J-Series Thruster Using Inert Gas," AIAA Paper No. 82-1929, November 1982.

TABLE I - Description of Neutralizer Geometries

NEUTRALIZER GEOMETRY	MECHANICAL MODIFICATION (from baseline)
#1	baseline design
#2	molybdenum orifice plate of exterior housing removed
#3	• molybdenum orifice plate removed • exterior housing removed from region of keeper • keeper shortened and enclosed with 0.47 cm dia. orifice
#4	• identical to geom #3, except for reduction in keeper orifice diameter to 0.33 cm

TABLE II - Nominal Thruster Conditions for Neutralizer Characterization

Condition	Performance Parameter			Operating Parameter			
	Input Power (W)	Thrust (mN)	Isp (s)	Accel Voltage, V_a (V)	Beam Voltage, V_b (V)	Beam Current, J_b (A)	Disch Propel Eff., η_{ud}
#1	670	30	2000	140	570	0.80	0.88
#2	1140	50	2440	170	700	1.20	0.92
#3	1620	70	2800	220	890	1.45	0.91

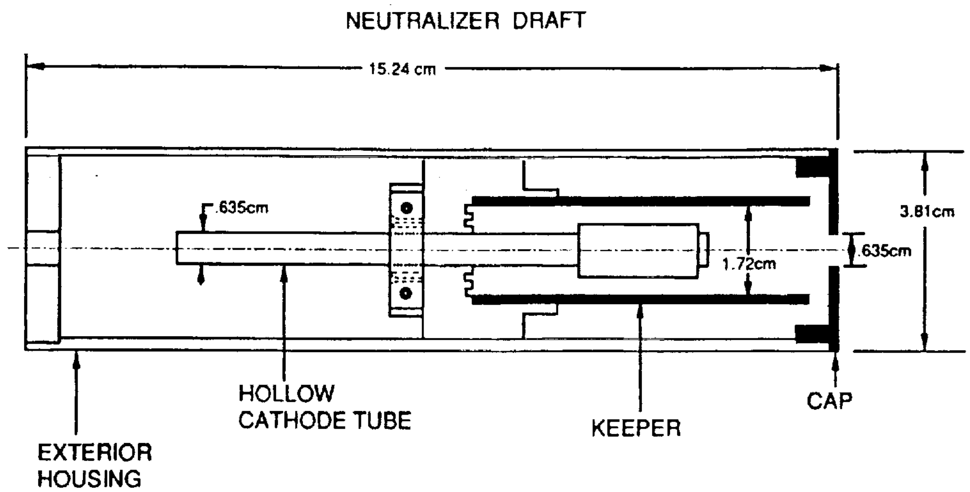

1a - Geometry #1; baseline design

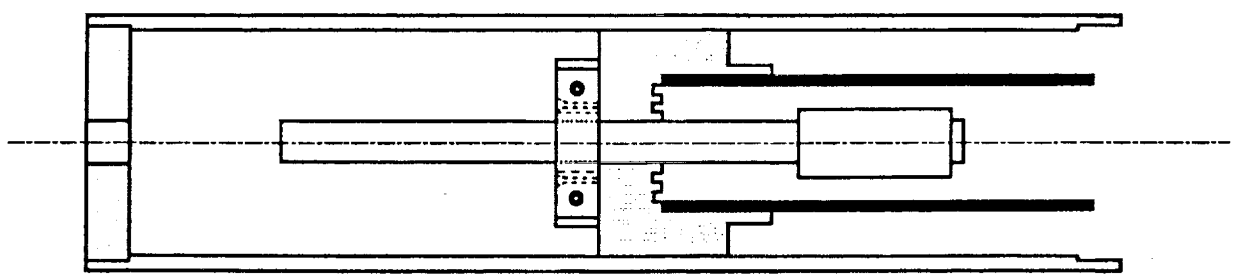

1b - Geometry #2

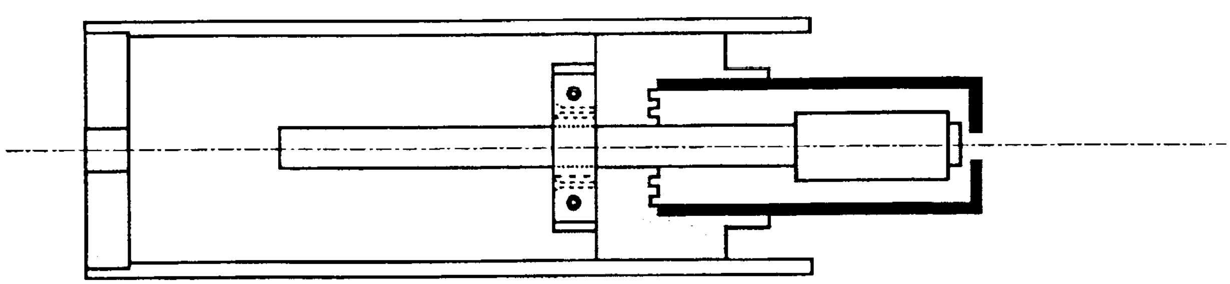

1c - Geometry #3

Fig. 1 Neutralizer mechanical designs.

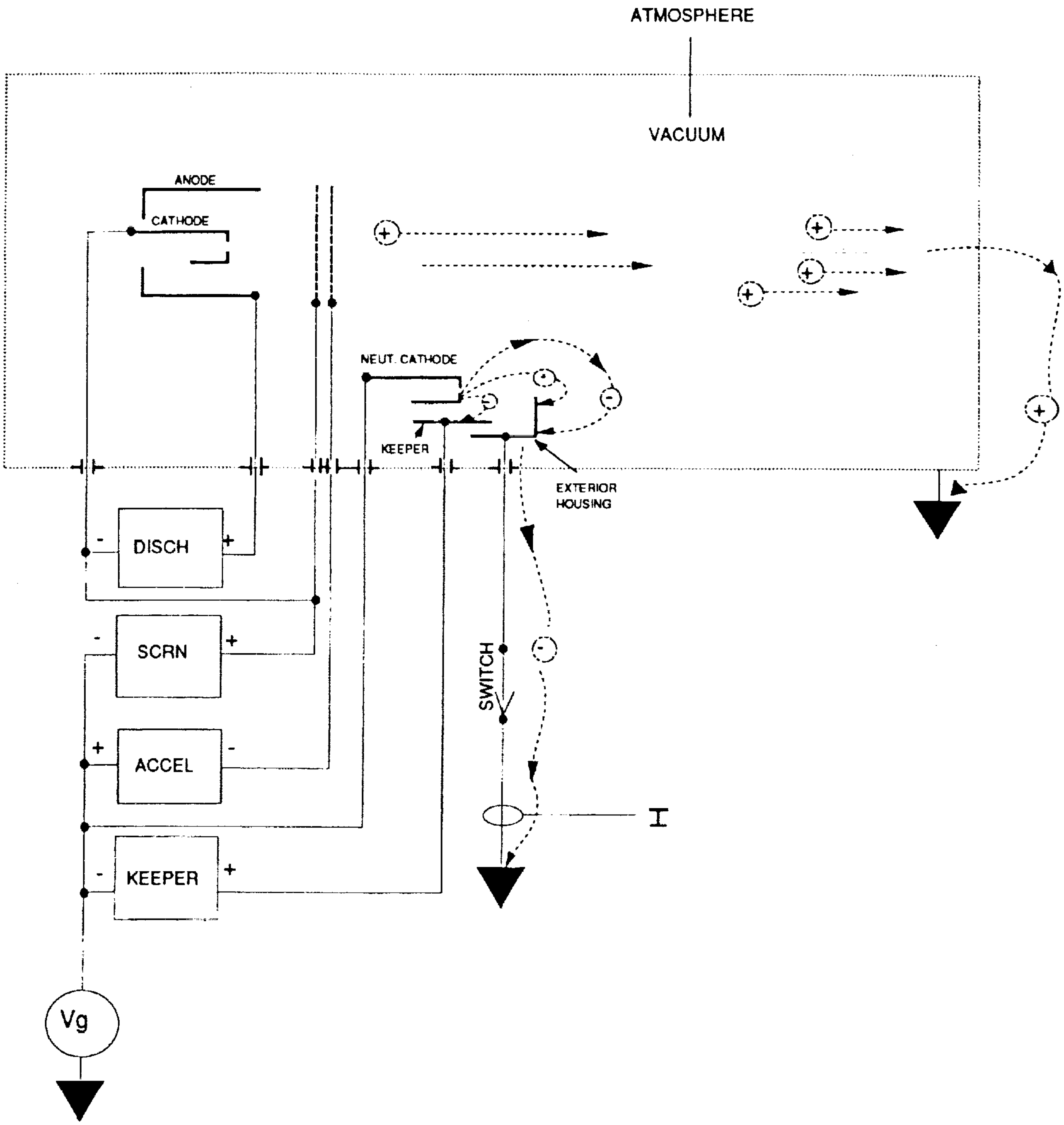

Fig. 2 Electrical schematic; grounded neutralizer exterior housing and plasma screen.

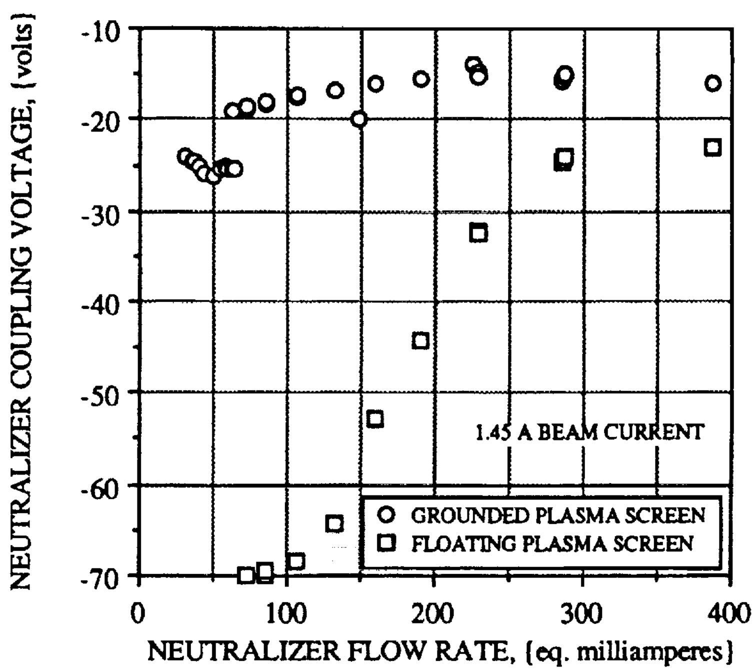

Fig. 3 Coupling voltage vs. flow rate for neutralizer geometry #1; grounded and ungrounded plasma screen and neutralizer exterior housing.

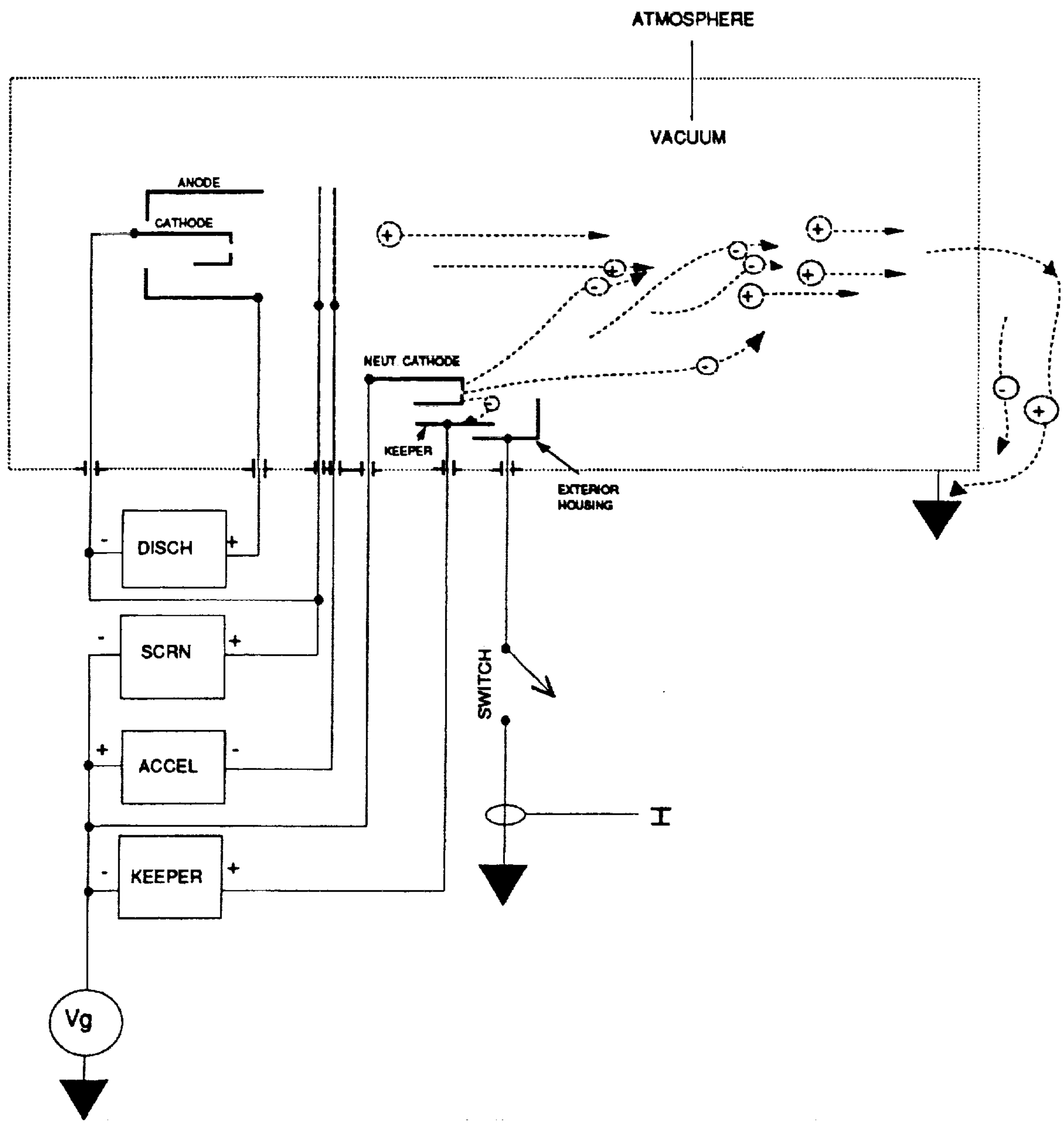

Fig. 4 Electrical schematic; floating neutralizer exterior housing and plasma screen.

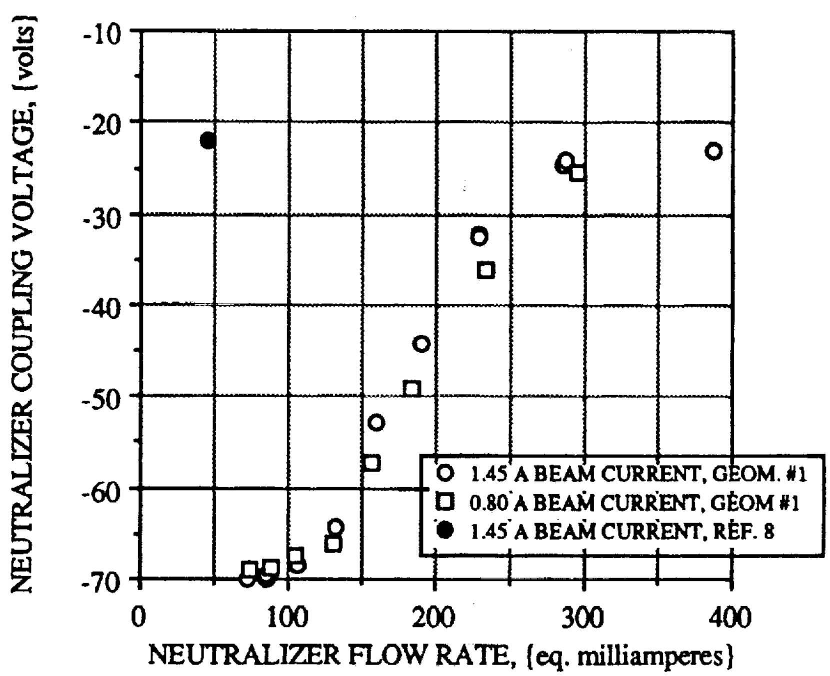

Fig. 5 Coupling voltage vs. flow rate; neutralizer geometry #1.

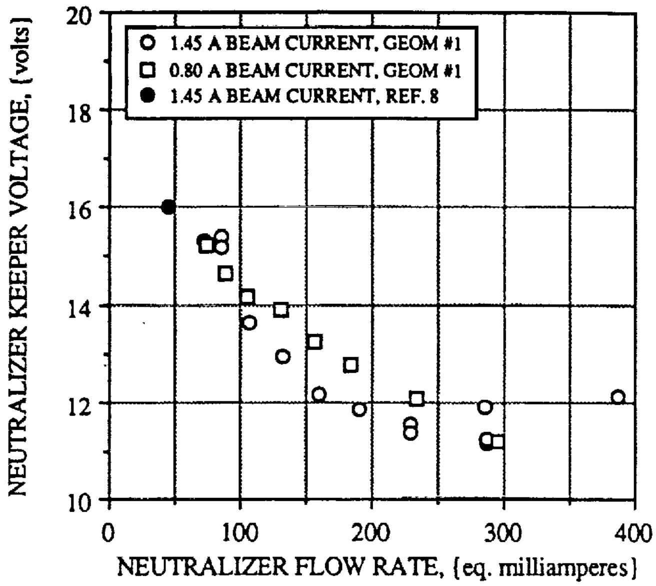

Fig. 6 Keeper voltage vs. flow rate; neutralizer geometry #1.

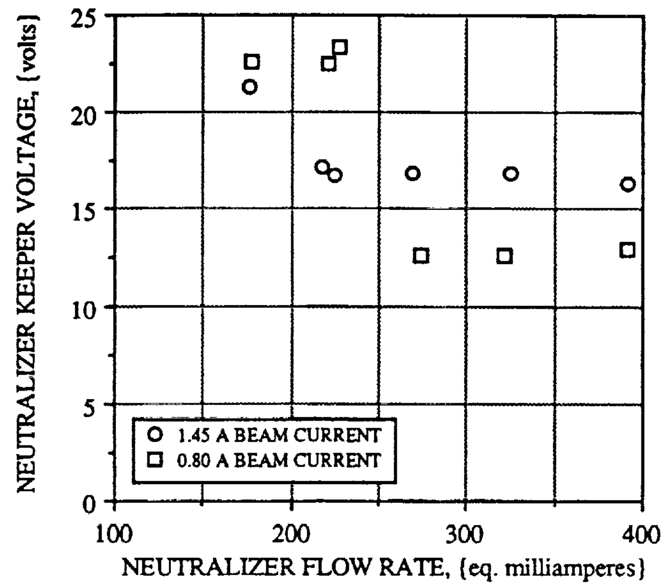

Fig. 8 Keeper voltage vs. flow rate; neutralizer geometry #2.

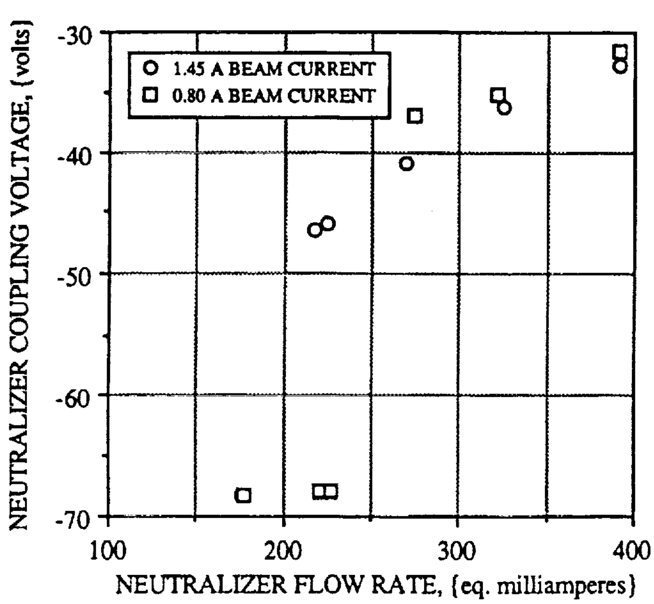

Fig. 7 Coupling voltage vs. flow rate; neutralizer geometry #2.

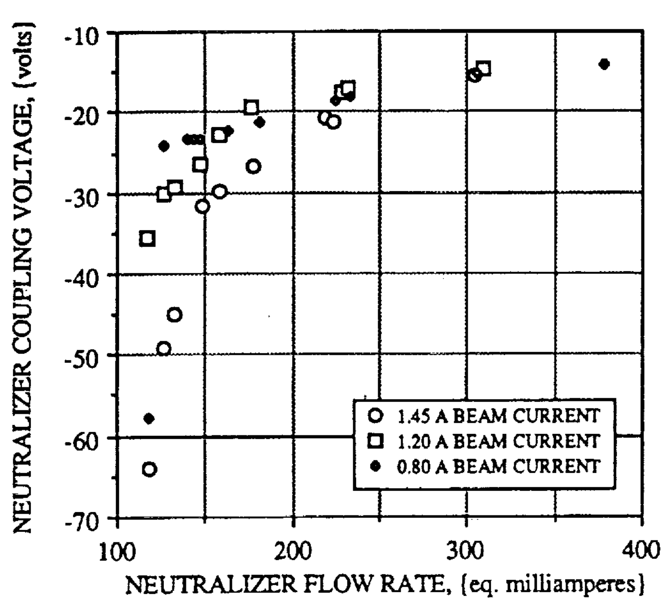

Fig. 9 Coupling voltage vs. flow rate; neutralizer geometry #3.

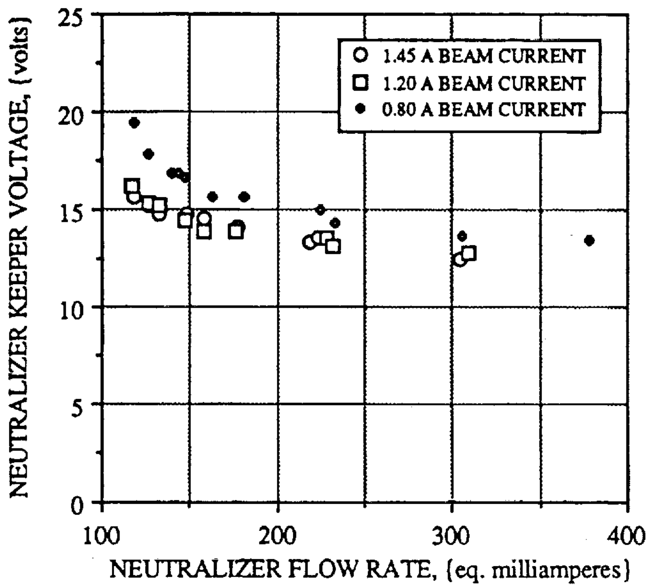

Fig. 10 Keeper voltage vs. flow rate; neutralizer geometry #3.

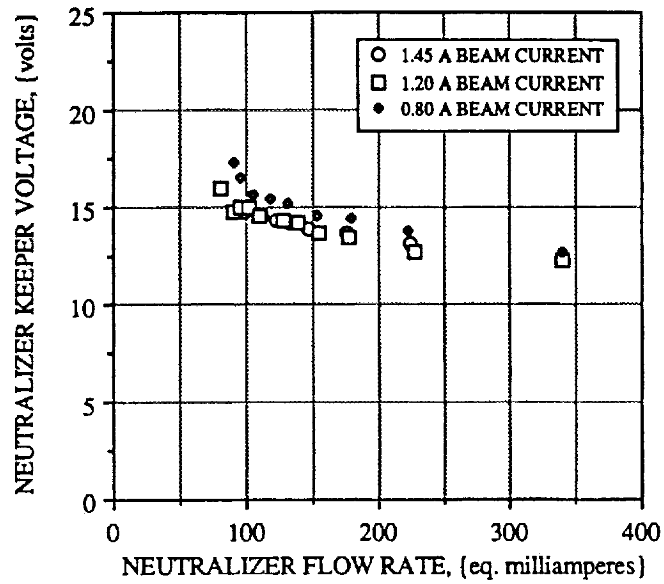

Fig. 12 Keeper voltage vs. flow rate; neutralizer geometry #4.

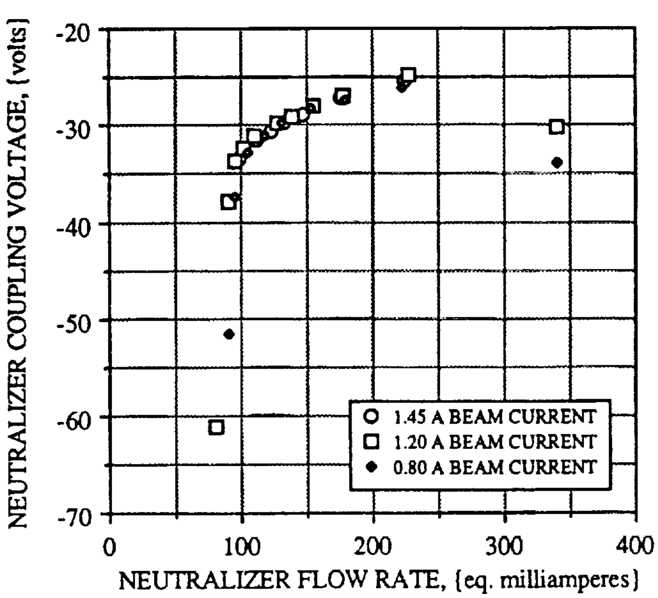

Fig. 11 Coupling voltage vs. flow rate; neutralizer geometry #4.

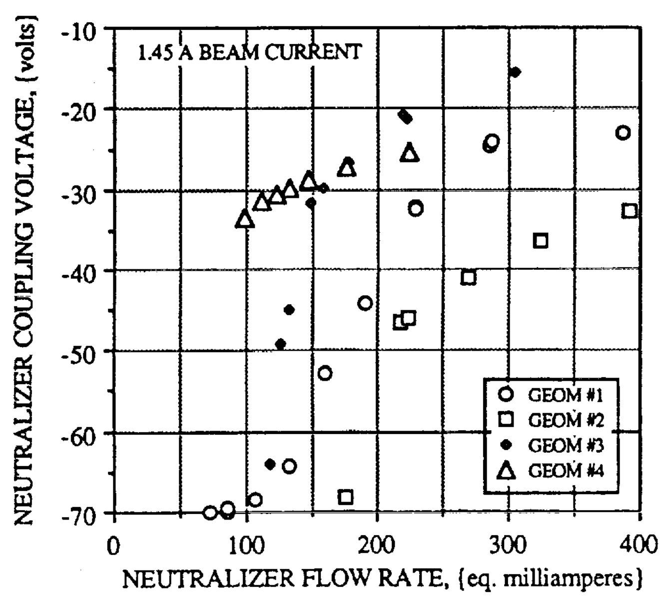

Fig. 13 Coupling voltage vs. flow rate comparison; 1.45 A beam current.

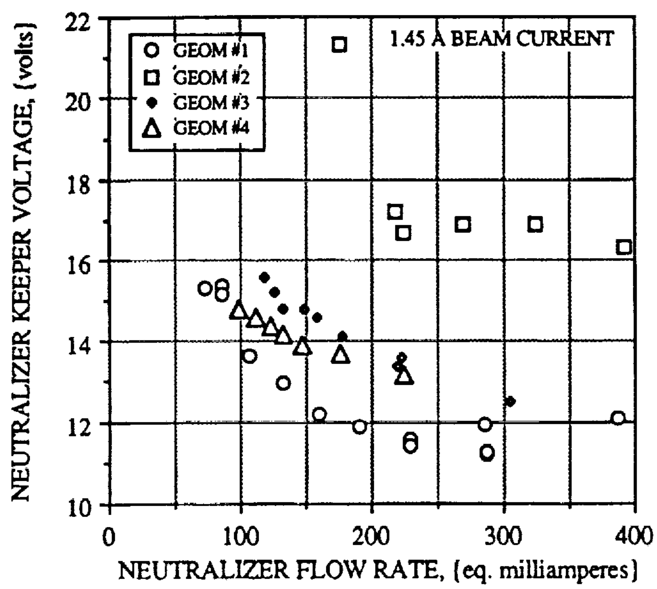

Fig. 14 Keeper voltage vs. flow rate comparison; 1.45 A beam current.

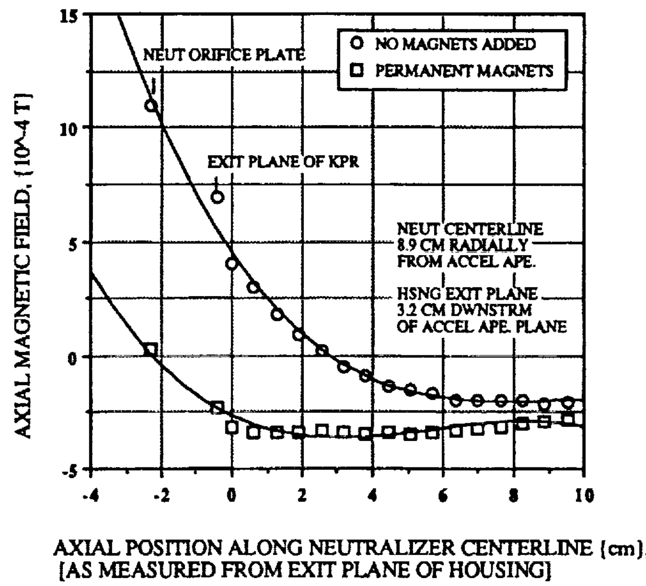

Fig. 16 Axial magnetic field component, with and without permanent magnets; neutralizer geometry #2, standard location.

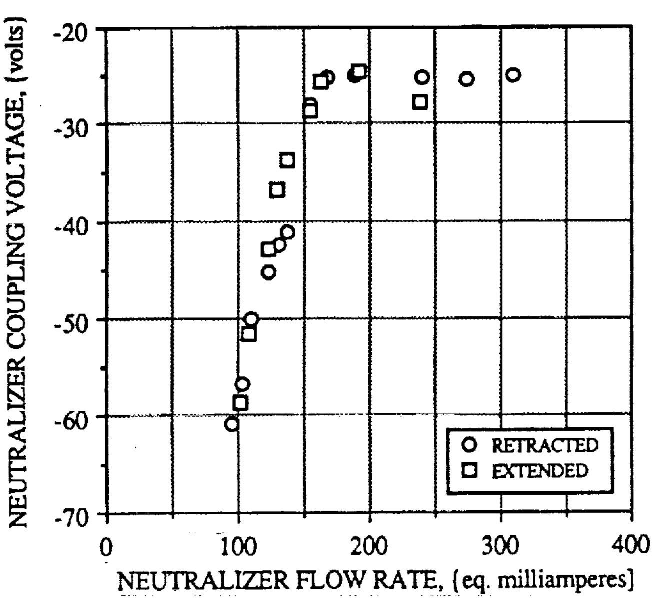

Fig. 15 Coupling voltage vs. axial position; geometry #1, 1.45 A beam current.

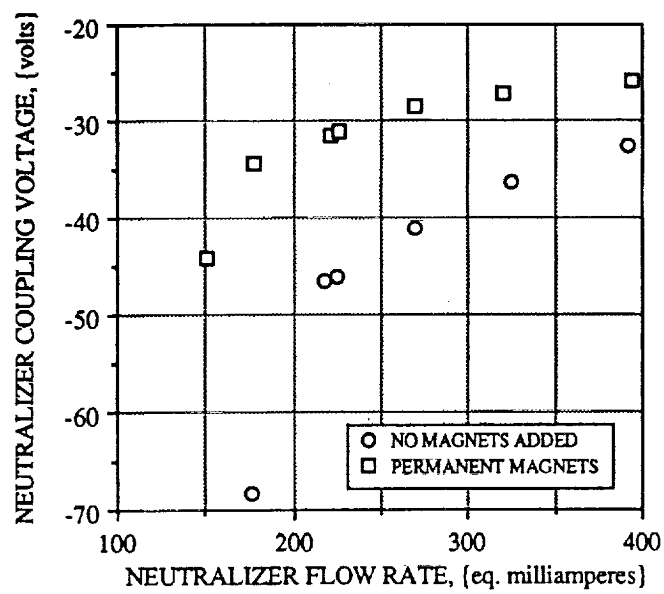

Fig. 17 Coupling voltage vs. flow rate, with and without permanent magnets; neutralizer geometry #2, 1.45 A beam current.

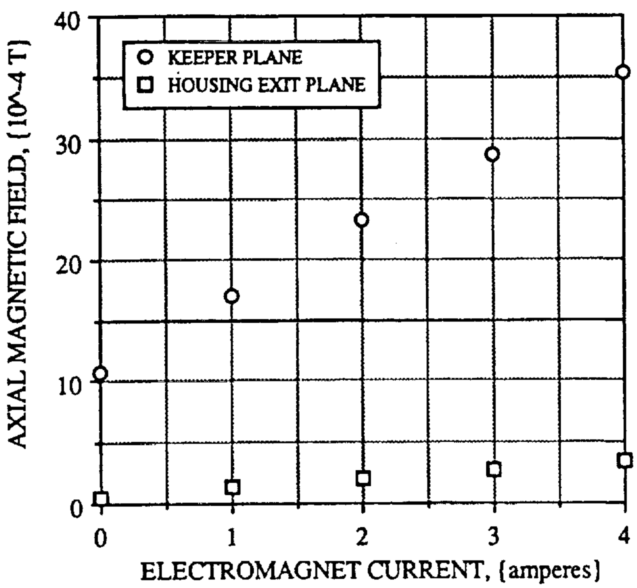

Fig. 18 Axial magnetic field vs. applied electromagnet current; neutralizer geometry #3.

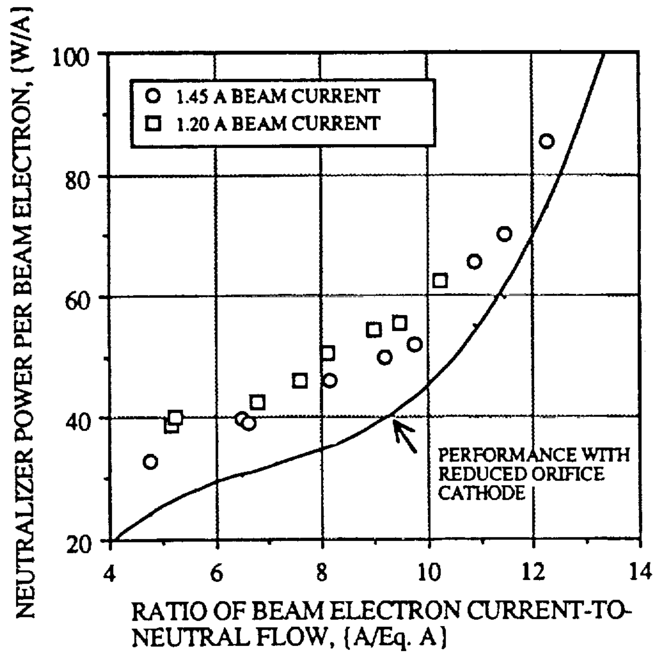

Fig. 20 Neutralizer geometry #3 performance characteristic.

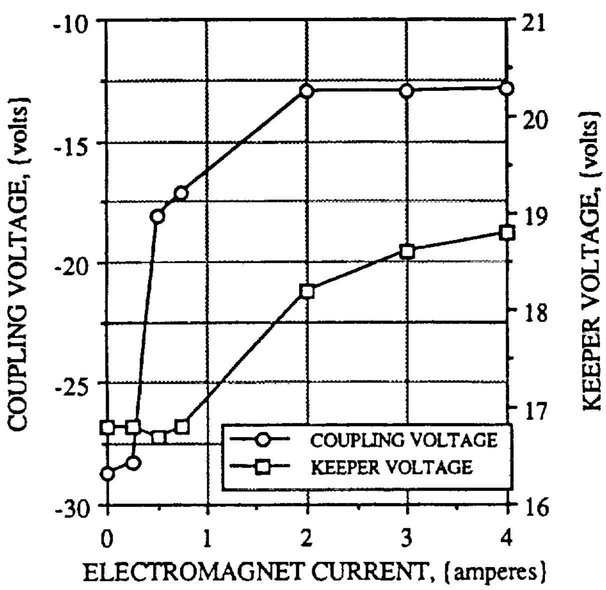

Fig. 19 Coupling and keeper voltages vs. applied electromagnet current; 1.45 A beam current, ~220 mA neutralizer flow rate, geometry #3.

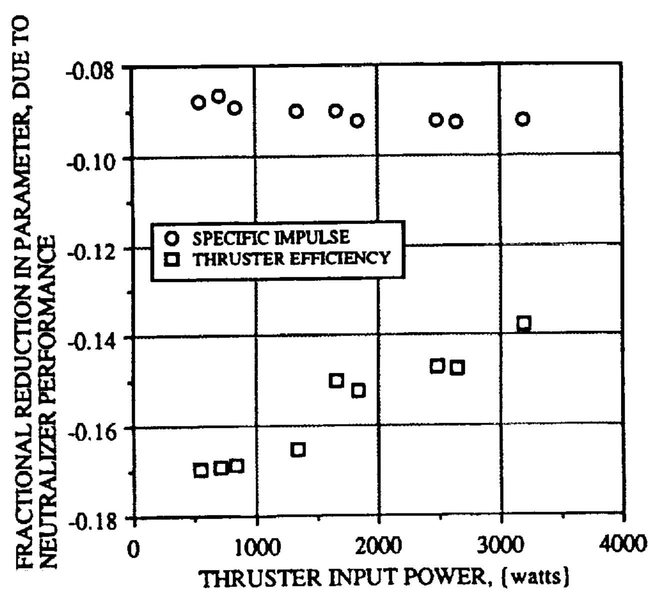

Fig. 21 Impact of neutralizer performance on thruster specific impulse and efficiency.

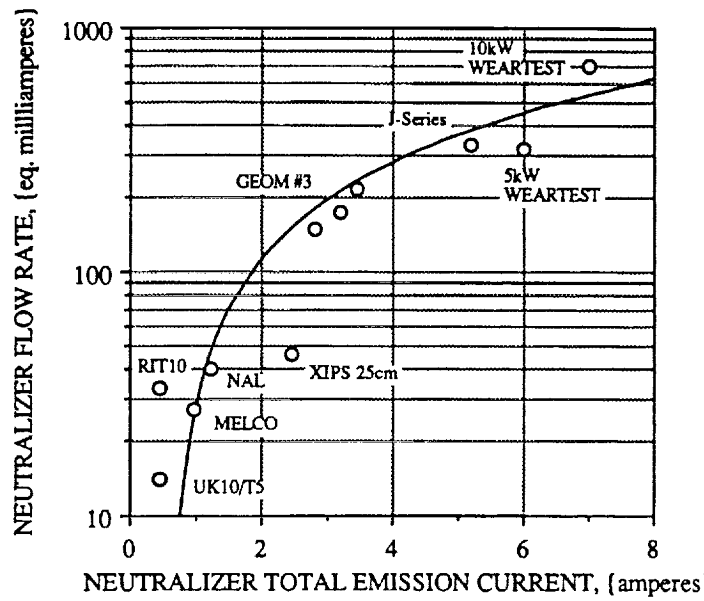

Fig. 22 Neutralizer flow rate vs. total emission current.

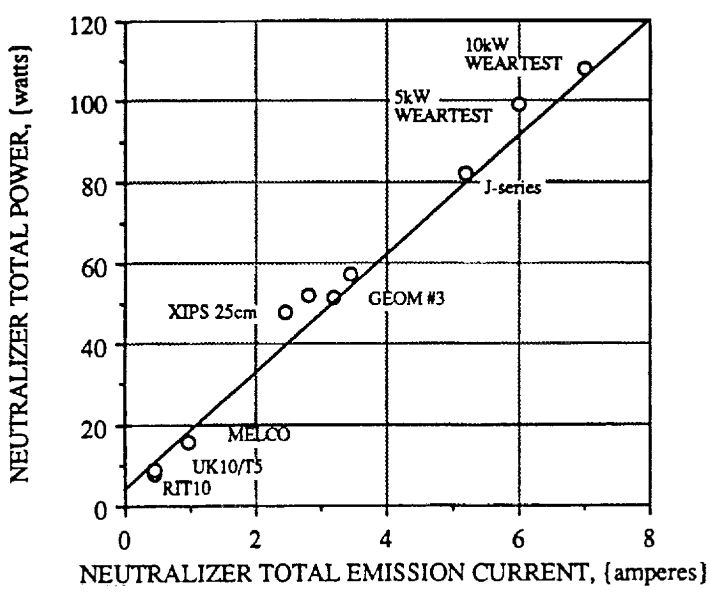

Fig. 23 Neutralizer power vs. total emission current.

REPORT DOCUMENTATION PAGE

Form Approved
OMB No. 0704-0188

1. AGENCY USE ONLY (*Leave blank*)	2. REPORT DATE	3. REPORT TYPE AND DATES COVERED
	October 1991	Technical Memorandum

4. TITLE AND SUBTITLE

Neutralizer Optimization

5. FUNDING NUMBERS

WU-506-42-31

6. AUTHOR(S)

Michael J. Patterson and Kayhan Mohajeri

7. PERFORMING ORGANIZATION NAME(S) AND ADDRESS(ES)

National Aeronautics and Space Administration
Lewis Research Center
Cleveland, Ohio 44135-3191

8. PERFORMING ORGANIZATION REPORT NUMBER

E-6903

9. SPONSORING/MONITORING AGENCY NAMES(S) AND ADDRESS(ES)

National Aeronautics and Space Administration
Washington, D.C. 20546-0001

10. SPONSORING/MONITORING AGENCY REPORT NUMBER

NASA TM-105578

11. SUPPLEMENTARY NOTES

Prepared for the 22nd International Electric Propulsion Conference cosponsored by the AIDAA, AIAA, DGLR, and JSASS. Viareggio, Italy, October 14–17, 1991. Michael J. Patterson, NASA Lewis Research Center and Kayhan Mohajeri, Department of Physics, Purdue University, West Lafayette, Indiana, 47907. Responsible person, Michael J. Patterson, (216) 433-7481.

12a. DISTRIBUTION/AVAILABILITY STATEMENT

Unclassified - Unlimited
Subject Category 20

12b. DISTRIBUTION CODE

13. ABSTRACT ***(Maximum 200 words)***

This paper discusses the preliminary results of a test program to optimize a neutralizer design for 30 cm xenon ion thrusters. The impact of neutralizer geometry, neutralizer axial location, and local magnetic fields on neutralizer performance is discussed. The effect of neutralizer performance on overall thruster performance is quantified, for thruster operation in the 0.5–3.2 kW power range. Additionally, these data are compared to data published for other NSSK and primary propulsion xenon ion thruster neutralizers.

14. SUBJECT TERMS

Ion thruster; Xenon ion propulsion; Auxiliary propulsion

15. NUMBER OF PAGES

20

16. PRICE CODE

A03

17. SECURITY CLASSIFICATION OF REPORT	18. SECURITY CLASSIFICATION OF THIS PAGE	19. SECURITY CLASSIFICATION OF ABSTRACT	20. LIMITATION OF ABSTRACT
Unclassified	Unclassified	Unclassified	